INSTITUTE OF PHYSICS PUBLISHING CLASSICAL AND QUANTUM GRAVITY

Class. Quantum Grav. **21** (2004) S487–S492 PII: S0264-9381(04)69087-3

Characterization of the LIGO 4 km Fabry–Perot cavities via their high-frequency dynamic responses to length and laser frequency variations

M Rakhmanov[1], F Bondu[2], O Debieu[2] and R L Savage Jr[3]

[1] Department of Physics, University of Florida, Gainesville, FL 32611, USA
[2] Observatoire de la Côte d'Azur, Nice, France
[3] LIGO Hanford Observatory, PO Box 159, Richland, WA 99352, USA

E-mail: malik@phys.ufl.edu

Received 14 September 2003
Published 3 February 2004
Online at stacks.iop.org/CQG/21/S487 (DOI: 10.1088/0264-9381/21/5/015)

Abstract

Recent measurements at the LIGO Hanford Observatory have confirmed the predicted high-frequency dynamic response of km scale Fabry–Perot cavities to length and laser frequency variations. The dynamic response functions have been exploited to determine a number of cavity parameters including the cavity length and the resonance width. A new technique based on a variation of these measurements has been utilized to measure the interferometer arm cavity lengths with a precision of 80 μm. We present an overview of these measurements and discuss how the dynamic field responses could be used to measure the cavity g factors which are related to the mirror radii of curvature.

PACS numbers: 04.80.Nn, 07.60.Ly, 42.60.Da, 95.55.Ym

(Some figures in this article are in colour only in the electronic version)

1. Introduction

To maintain resonance in a Fabry–Perot cavity when the cavity length, L, and laser frequency, ω, are varying, the dynamic resonance condition,

$$\frac{\delta\tilde{L}(s)}{L} = -C(s)\frac{\delta\tilde{\omega}(s)}{\omega}, \qquad \text{where} \quad C(s) = \frac{1-\mathrm{e}^{-2sT}}{2sT}, \tag{1}$$

must be satisfied [1]. Here T is the light transit time in the cavity, s is the Laplace-domain variable, and $C(s)$ is the laser-frequency-to-length transfer function. Deviations from this resonant state are typically sensed by the Pound–Drever–Hall (PDH) locking signal, V. For small deviations from resonance, the responses of the PDH signal to variations in the laser frequency and the cavity length are given by the transfer functions

$$H_L(s) = \frac{\delta\tilde{V}(s)}{\delta\tilde{L}(s)} \qquad \text{and} \qquad H_\omega(s) = \frac{\delta\tilde{V}(s)}{\delta\tilde{\omega}(s)}. \tag{2}$$

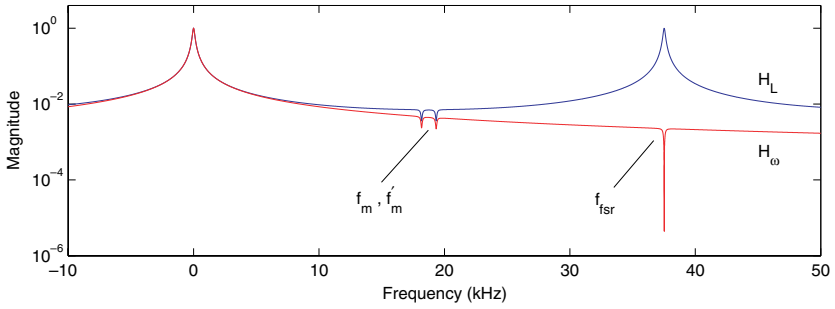

Figure 1. Predicted magnitudes of $H_L(s)$ and $H_\omega(s)$. The features labelled f_m and f'_m are discussed in section 3.

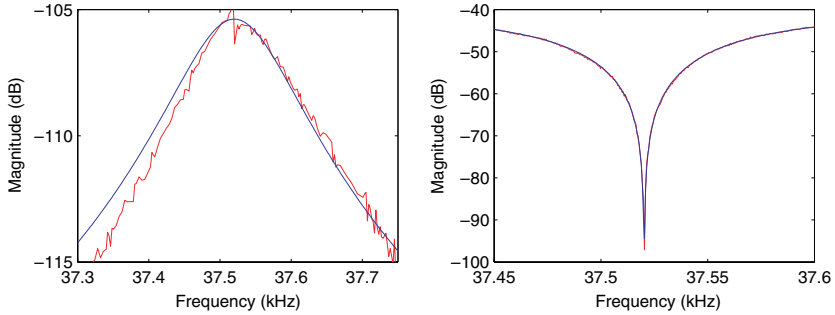

Figure 2. Measured magnitudes of $H_L(s)$ (left) and $H_\omega(s)$ (right) and the theoretical predictions (almost indistinguishable for $H_\omega(s)$).

Using the LIGO 4 km arm cavity parameters, the predicted magnitudes of these transfer functions are plotted over a 50 kHz span in figure 1. The response to length variations, $H_L(s)$, peaks at integer multiples of the cavity free spectral range frequency, $f_{\rm fsr}$,[4] and the halfwidth of the peaks (HWHM) equals the commonly quoted 'cavity pole' frequency. The response to laser frequency variations, $H_\omega(s)$, goes to zero at multiples of $f_{\rm fsr}$.

2. Response near multiples of $f_{\rm fsr}$

To measure $H_\omega(s)$ we vary the frequency of the laser light incident on the cavity; for $H_L(s)$ we vary the position of the input mirror of the cavity. The PDH signals are measured at the anti-symmetric port of the interferometer. Precise calibration of the excitation and PDH modulation frequencies is achieved via a benchtop rubidium frequency standard (SRS FS725). All $H_\omega(s)$ measurements are performed in a one-arm configuration with the second arm cavity mirrors and the recycling mirror misaligned. The full power-recycled interferometer is required only for $H_L(s)$ measurements in order to acquire sufficient signal to noise ratio.

Considering only the dynamic carrier field in the cavity [1], the transfer functions are given explicitly by

$$H_L(s) = \frac{1 - r_a r_b}{1 - r_a r_b \, \mathrm{e}^{-2sT}} \qquad \text{and} \qquad H_\omega(s) = C(s) H_L(s), \tag{3}$$

[4] The high-frequency response to gravitational waves is different from the response at dc [2]. For an optimally-oriented source the response is functionally equivalent to $H_\omega(s)$. However, for other orientations, the averaged response at $f_{\rm fsr}$ is only about a factor of five lower than the averaged response at dc. Searches for gravitational waves at $f_{\rm fsr}$ are being considered (see Markowicz *et al* [3]).

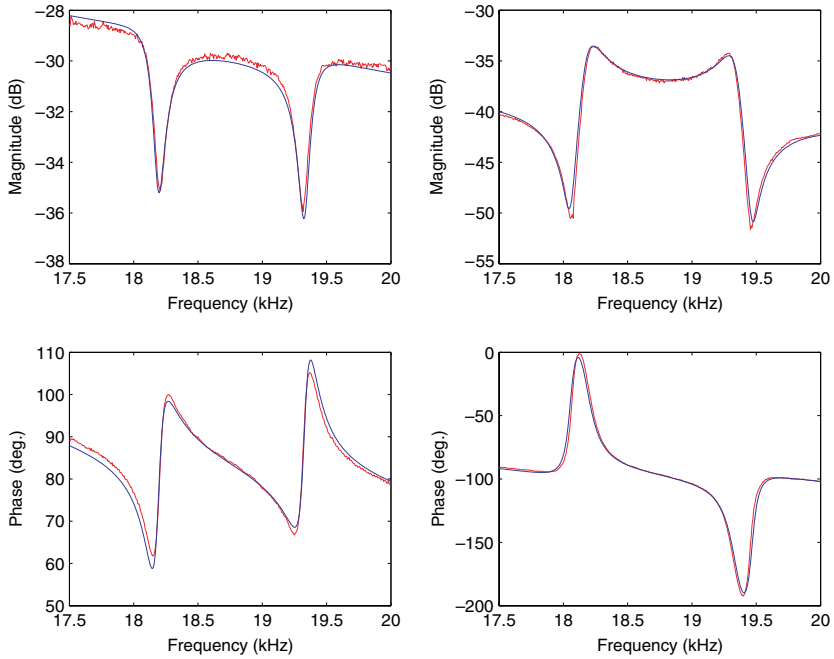

Figure 3. Bode plots of $H_\omega(s)$ measured near frequencies f_m (18.18 kHz) and f'_m (19.34 kHz) for demodulation phases of -18° (left) and $+73^\circ$ (right). The smooth curves are the theoretical predictions.

where $r_{a,b}$ are the cavity mirror reflectivities. The magnitudes of $H_L(s)$ and $H_\omega(s)$, measured near $f_{\rm fsr}$ (≈ 37.52 kHz), are shown in figure 2 along with the theoretical predictions of equation (3) multiplied by a constant scale factor. The peak in $H_L(s)$ at $f_{\rm fsr}$ is observed with the expected width (FWHM) of approximately 164 Hz. The cusp in $H_\omega(s)$ confirms the insensitivity of the cavity to variations of the laser frequency at $f_{\rm fsr}$. The location of the cusp yields the value of $f_{\rm fsr}$ within 10 mHz and thus the cavity length with a precision of 1 mm.

3. Response near sideband-related frequencies

The PDH sidebands are generated by phase modulation at $f_{\rm mod} = 24.481\,326$ MHz, and thus are symmetrically spaced many free spectral ranges from the resonant carrier. Because of the periodic nature of Fabry–Perot cavities, features in $H_\omega(s)$ are generated when the frequency of the laser frequency modulation coupled with the sideband frequency enforces *dynamic* resonance of the sideband light in the cavity [4]. The lowest frequency pair of these features appear at

$$f_m = f_{\rm mod} - N f_{\rm fsr} \qquad \text{and} \qquad f'_m = (N+1) f_{\rm fsr} - f_{\rm mod}, \tag{4}$$

where $N = \text{integer}(f_{\rm mod}/f_{\rm fsr}) = 652$. Bode plots of $H_\omega(s)$ measured near f_m and f'_m are shown in figure 3. The theory curves are given by

$$H_\omega(s) = C(s)\left(\frac{a_0}{1 - q_0\,\mathrm{e}^{-2sT}} - \frac{a_1}{1 - q_1\,\mathrm{e}^{-2sT}} - \frac{a_1^*}{1 - q_1^*\,\mathrm{e}^{-2sT}}\right). \tag{5}$$

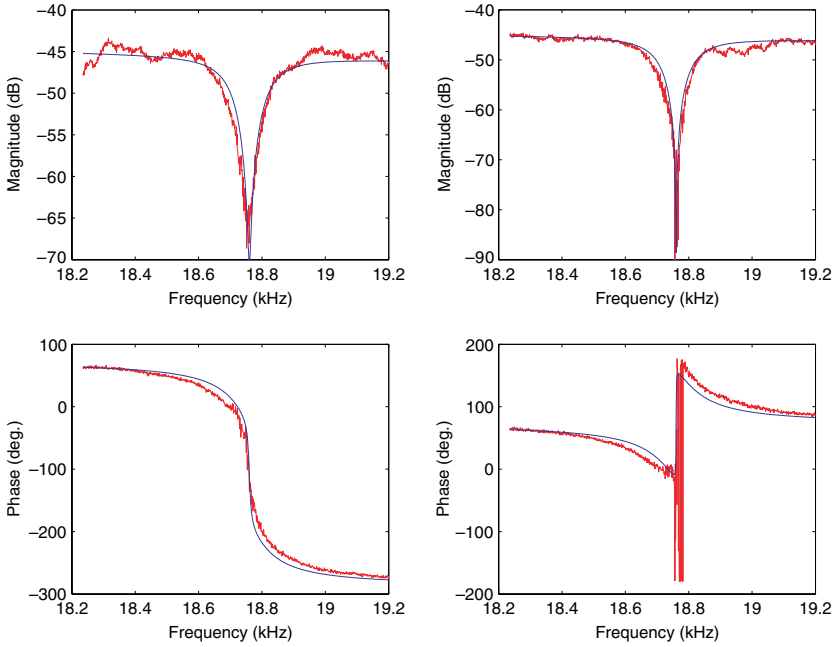

Figure 4. Bode plots of $H_\omega(s)$ (quadrature channel) measured near $f_{\rm fsr}/2$ for $f_{\rm mod} = 24\,482\,153$ Hz (left) and $f_{\rm mod} = 24\,482\,154$ Hz (right).

This expression includes the effect of the dynamic sideband fields in the cavity [4]. The coefficients, a_n, depend on mirror reflectivities and the demodulation phase[5], and $q_n = r_a r_b \exp(-4{\rm i}\pi n f_{\rm mod} T)$. Although the features at f_m and f'_m are not as sharp as the cusps at multiples of $f_{\rm fsr}$, the large value of N enables precision measurement of the cavity length by observing the $f'_m - f_m$ frequency separation. This spacing is given by $\Delta f_m = (2N+1) f_{\rm fsr} - 2 f_{\rm mod}$ so the length measurement precision is given by $\delta L/L = \delta(\Delta f_m)/[(2N+1) f_{\rm fsr}]$. Thus determination of the frequency separation with 12 Hz precision constrains the cavity length with 1 mm precision. This is comparable to the precision achieved by localizing the cusp in $H_\omega(s)$ near $f_{\rm fsr}$.

4. Precision measurement of arm cavity lengths

By adjusting $f_{\rm mod}$ so that the two sideband related features converge at $f_m = f'_m = f_{\rm fsr}/2$, we are able to improve the precision of the cavity length measurement by more than an order of magnitude [5]. The precision of the measurement is presently limited by the minimum step size (1 Hz) for setting the frequency of the modulation source. In practice, we observe the abrupt change in the trajectory of the phase of $H_\omega(s)$ as $f_{\rm mod}$ is tuned across the $f'_{\rm mod} = (N+1/2) f_{\rm fsr}$ point. Figure 4 shows Bode plots of $H_\omega(s)$ as $f_{\rm mod}$ is incremented by 1 Hz from below the $f'_{\rm mod}$ point (left) to above the $f'_{\rm mod}$ point (right). Note the dramatic change in the phase trajectory from monotonic roll-off to a roll-off with an abrupt 180° step. We therefore determine $f'_{\rm mod}$ within ±0.5 Hz which constrains the cavity lengths to within ±80 μm. The interferometer

[5] The coefficients, a_n, are given by $a_0 = (e^{i\gamma}\rho_1 + e^{-i\gamma}\rho_1^*)q_0/(1-q_0)$, and $a_1 = e^{i\gamma}\rho_0 q_1/(1-q_1)$, where $\rho_n = r_a - (t_a^2/r_a)q_n/(1-q_n)$ is the static cavity reflectivity with $n = 0$ for the carrier field and $n = 1$ for the sideband fields.

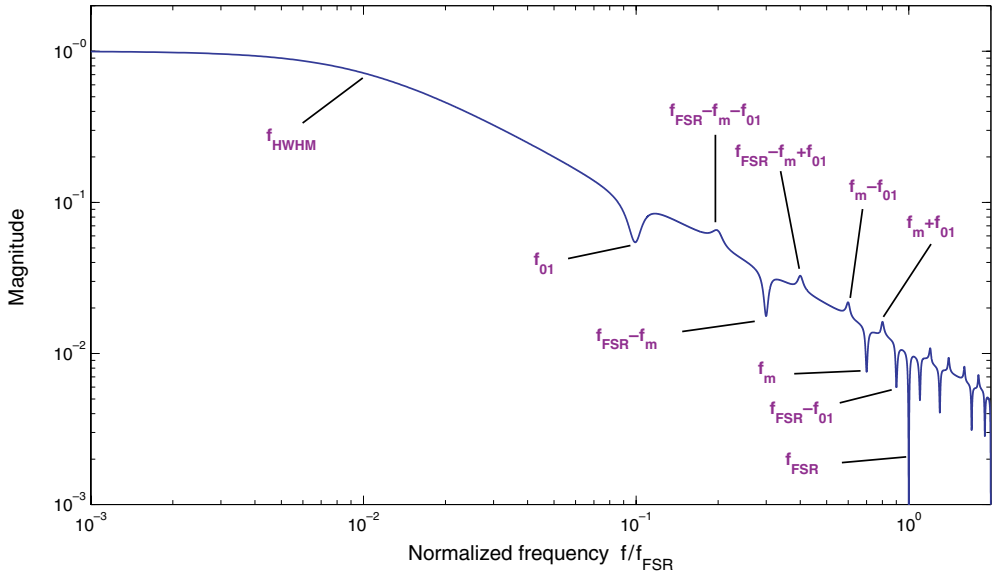

Figure 5. Calculated magnitude of $H_\omega(s)$ for a misaligned cavity with $f_m = 0.7 f_{\rm fsr}$ and $f_{01} = 0.1 f_{\rm fsr}$.

arm lengths thus measured are $L_X = 3995.084\,18 \pm 0.000\,08$ m and $L_Y = 3995.044\,37 \pm 0.000\,08$ m.

5. Measurement of the cavity g factor

When the incident laser beam is offset or misaligned with respect to the cavity axis, $H_\omega(s)$ acquires additional features at frequencies related to the higher-order transverse mode separation, f_{01}. This spacing is directly related to the mirror radii of curvature, $R_{1,2}$, by $f_{01} = f_{\rm fsr} \arccos(\sqrt{g_1 g_2})/\pi$, where $g_{1,2} = 1 - L/R_{1,2}$. Therefore, measuring $H_\omega(s)$ for a misaligned cavity would allow us to determine the cavity g factor product which is directly related to the mirror radii of curvature [6]. Figure 5 shows an example of $H_\omega(s)$ for a misaligned cavity. Although the cavity is locked on the $\rm TEM_{00}$ spatial mode, the $\rm TEM_{01}$ mode will *dynamically* resonate at laser frequency modulation frequencies where the residual round trip phase coupled with the Gouy phase change for the higher-order mode is an integer multiple of 2π.

Instead of making a swept sine measurement, an error signal can be generated by adding phase modulation sidebands at $N' f_{\rm fsr} + f_{01}$ and demodulating at this frequency. When a monolithic photodiode is used, the magnitude of the error signal is proportional to the square of the fractional misalignment but with a split photodiode it is proportional to the misalignment to first order. This error signal could be utilized to monitor changes in the mirror radii of curvature during variations in the thermal loading, for example immediately after acquiring lock.

6. Effect of arm-length mismatch

The magnitude of $H_L(s)$ shown in figure 2 has a small feature near the peak which is resolved in figure 6. This feature does not result from the dynamics of a single Fabry–Perot cavity;

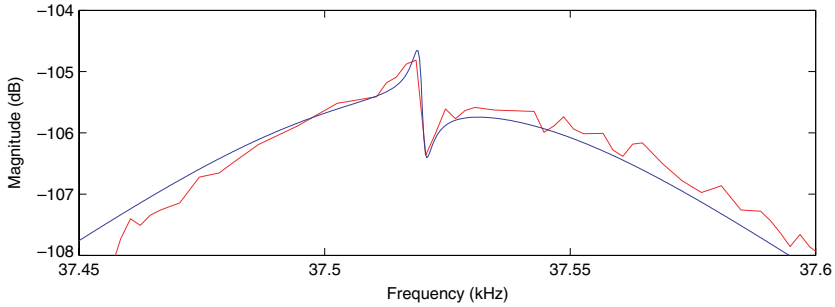

Figure 6. Magnitude of $H_L(s)$ near f_{fsr}. The smooth curve is generated by *Finesse* for a 4 cm arm length mismatch with the Y-arm being shorter than the X-arm.

it appears only when the interferometer is operating in the full power-recycled configuration. The effect occurs because modulation of the length of one arm produces simultaneous excitation of the common and differential modes of the interferometer. The common mode is then amplified in the recycling cavity and a small fraction of it leaks into the anti-symmetric port due to asymmetries.

Modelling with the *Finesse* software package [7] indicates that the feature in $H_L(s)$ results from a 4 cm difference in the lengths of the interferometer arms (smooth curve in figure 6). The precision length measurements described above confirm both the sign and magnitude of this predicted arm cavity length difference.

Acknowledgments

We thank G Mueller for assistance with *Finesse* and the whole LIGO team for constructing and operating the interferometers that enabled this work. This material is based upon work supported by the US National Science Foundation under Cooperative Agreements no PHY-0107417 and PHY-0244902, and by the CNRS in France. This document has been assigned LIGO Laboratory document number LIGO-P030044-00-W.

References

[1] Rakhmanov M, Savage R L Jr, Reitze D H and Tanner D B 2002 *Phys. Lett.* A **305** 239
[2] Sigg D 2003 Strain calibration in LIGO *LIGO Technical Document T970101-B-D*
[3] Markowicz J, Savage R and Schwinberg P 2003 Development of a readout scheme for high-frequency gravitational waves *LIGO Technical Document T030186-00-W*
[4] Savage R L Jr, Rakhmanov M and Bondu F 2003 Observation of dynamic resonance in a kilometer-scale Fabry-Perot cavity *LIGO Document P020031-00-W* in preparation for submission to *Phys. Lett.* A
[5] An even more precise technique has been reported by Araya A *et al* 1999 *Appl. Opt.* **38** 2848
[6] Debieu O 2003 Détermination de méthodes de mesure précise des modes dans une cavite Fabry–Perot *Rapport de stage de DEA* Université de Nice Sophia-Antipolis et Observatoire de la Côte d'Azur
[7] Freise A *et al* 2004 Frequency domain interferometer simulations including higher order spatial modes *Class. Quantum Grav.* **21** S1067